

Electrochemical Corrosion Behaviour of Nano Aluminium - Polytetrafluoroethylene Pigment Modified Water borne Epoxy Coating on Carbon Steel

Mingshuai Guo¹, Qingyang Zeng¹, Xiaoting Ren¹, Lili Xue^{1,*}, Yonglei Xin^{2,*}, Yueming Ren¹, Likun Xu², Li Li¹

¹ Center for Biomedical Materials and Engineering, Institute of Materials Processing and Intelligent Manufacturing, College of Materials Science and Chemical Engineering, Harbin Engineering University, 145 Nantong Street, Harbin City, Heilongjiang Province, 150001, P.R. China

² State Key Laboratory for Marine Corrosion and Protection, Luoyang Ship Material Research Institute (LSMRI), Qingdao, 266237, P.R. China

*E-mail: xinyi@sunrui.net; xuelili@hrbeu.edu.cn

Received: 27 August 2020 / Accepted: 3 November 2020 / Published: 30 November 2020

For fasteners, corrosion causes rust on the threads, reduces their strength and making their disassembly difficult. The protective coating of fasteners needs to have excellent anti-corrosion and lubricating properties. In this paper, nano Aluminium (nano-Al) and Polytetrafluoroethylene (PTFE) particles were used to fabricate a nano Al-PTFE epoxy self-stratifying structure coating. The SEM, AFM, and DSC results show that the coating formed a self-stratifying structure when it is pre-dried at 110°C and then dried at 200°C. PTFE is located on the surface of the coating to enhance lubricity, while nano-Al is located at the bottom of the coating to enhance corrosion resistance. Moreover, Electrochemical impedance spectroscopy (EIS) shows that the C_{dl} of the nano Al-PTFE modified coating with an artificial defect is lower, while its R_{ct} is higher than that of the other two coatings, indicating that corrosive electrochemical activity only occurred in a small area of the coating. The SVET results indicate that the distance of the nano Al-PTFE modified coating from the defect edge contour only changed a little after 48 h of immersion. In conclusion, the coating has good anti-corrosion performance.

Keywords: Corrosion behaviour; Nano Al-PTFE; Self-stratifying; EIS; SVET

1. INTRODUCTION

Organic coating is one of the most widely applied methods for corrosion protection of metallic materials [1-3]. The protective effects of organic coatings on metal mainly include shielding effect [4], cathodic protection [5], pigment passivation [6] and corrosion inhibition [7]. However, even if the coating reaches an ideal state, there are still many transmission channels through which external media

can still penetrate through the coating. Due to the presence of water molecules at the interface between the organic coating and metal, the coating is continuously reduced in size due to water adhesion, weakening its protective performance [8]. Electrochemical impedance spectroscopy (EIS) can detect corrosion electrochemical signals of coating/metal system in situ and non-destructively [9], including measurements of coating capacitance (C_c), coating metal interface double-layer capacitance (C_{dl}) and other electrochemical parameters related to coating performance and failure. EIS can continuously and rapidly monitor corrosion in low-conductive media without the influence of a coating's strong ohmic drop, and obtain information about water permeability into the coating [10], ion diffusion [11], formation of blisters [12] and loss of adhesion [13], etc., to understand the corrosion mechanism of metals under coatings. Chen et al.[14] used absolute ethanol to extract coconut leaf extract and, using the EIS technique, determined that coconut leaf extracts exhibited excellent corrosion inhibition performance. Wan et al.[15] reported that the Sn-Ni alloy has excellent anti-corrosion properties compared to a pure Sn coating by using the EIS technique. Zhang et al.[16] also used EIS technique to demonstrate that the deposition of a superhydrophobic polypropylene coating on the AZ31 magnesium alloy surface effectively inhibits the corrosion process. The EIS technique helps obtain the average electrochemical information of the coating/metal system; however, corrosion usually starts in the local area. Therefore, the EIS technique needs to be used in combination with other detection technologies when studying the corrosion characteristics of coating/metal systems. Scanning vibrating electrode technology (SVET) can make up for the deficiency of traditional electrochemical technology, and monitor in situ the potential change of local corrosion as a result of electrochemical reaction of a defective coating/metal interface [17]. As for the relationship between potential and time, SVET can determine the rate of electrochemical reaction at the coating metal interface, which can provide a deeper understanding of the mechanism and influencing factors of coating stripping [18].

Fasteners used in marine environments are highly susceptible to corrosion by seawater and marine atmospheric media during service, and suffer varying degrees of wear during installation, removal and usage. The most common anti-corrosion coatings do not have sufficient mechanical strength and wear resistance, and are easily worn and damaged by mechanical influence. Then, they peel off quickly and fail to protect the substrate metals. Therefore, to achieve excellent corrosion resistance, the fastener's protective coating must have good mechanical wear resistance. When the compatibility of the filler with the film-forming resin is poor, the wear resistance and corrosion resistance of the coating can be difficult to balance. Increasing the wear resistance of the coating often comes at the expense of its corrosion resistance, resulting in a reduction in the coating protection life.

Polytetrafluoroethylene (PTFE) is widely used in wear-resistant coatings because of its self-lubricating properties. In our previous work [19], we added PTFE particles into a waterborne epoxy (EP) resin to realise lubrication as well as the anti-corrosive property. However, investigations of the electrochemical behaviour of metal coatings and the analysis of the coating microstructure revealed that PTFE particles and the waterborne epoxy resin have poor compatibility leading to a significant reduction of the corrosion resistance of the coating. In this paper, we prepared nano Al-PTFE composite pigments to modify the waterborne epoxy coating for purposes of enhancing its corrosion resistance. Furthermore, the corrosion electrochemical behaviour of the coating carbon steel system was investigated deeply by

using both the EIS and SVET techniques to understand the effects of nano Al-PTFE composite pigments on the corrosion resistance of the coating.

2. EXPERIMENTATION

2.1 Coating preparation

In this study, the self-stratification concept [20] was introduced to design the coating formulation. The substrate was Q235 carbon steel of size 60 mm × 60 mm × 10 mm. Before spraying, the steel was pretreated by sandblasting to ensure surface cleanliness. Then, the nano Al powder (developed by Shanghai Pantian Powder Material Co., Ltd.) was dissolved into distilled water, and ultrasonically dispersed for 1 h. The dispersed nano Al powder slurry was then added to the PTFE emulsion (developed by Kunshan Qixin Guanteng Plastic Chemical Co., Ltd.), and ultrasonic dispersed for 3 h. Since the surface energy of nano Al particles is extremely high, while the surface energy of the PTFE is extremely low, the two pigment composites tend to separate into two layers. Therefore, a surfactant was added to increase the miscibility of the slurry and to adjust viscosity to prevent pigment particles from precipitation during the ultrasonic dispersion process. The nano Al pigment and the composite pigments of nano Al powder 1wt.% and PTFE 6wt.% were added into the water-based epoxy resin (developed by Qingdao Marine Chemical Research Institute, China), respectively. Then, the anti-foaming agent, wetting agent, leveling agent and flash-rust inhibitor (the above 4 materials are all developed by Foshan Wengkaier Trading Co., Ltd.) were added into the composite water-based epoxy paint during the ultrasonic dispersion process, and mechanically stirred for 20 min. The steel sheets were then successively painted with the water-based epoxy coating, the nano Al modified waterborne epoxy coating and the nano Al-PTFE modified waterborne epoxy coating for a total of 5 times.

2.2 Characterisation

2.2.1 Electrochemical impedance spectroscopy (EIS)

The EIS measurement was taken using the IM6 electrochemical workstation, originally from ZAHNER Elektrik-GmbH&Co. of Germany. The experiment used a three-electrode system. The reference electrode was a saturated calomel electrode (SCE), the coating sample was the working electrode, and the auxiliary electrode was a Pt wire. The test was carried out with an open circuit potential at a test frequency range of 10 mHz to 100 kHz, and with a sinusoidal ac excitation signal of 20 mV, and a sample working area of 9.08 cm². The experimental data were fitted on the basis of equivalent electrical circuits using commercial software, Zsimpwin 3.21.

2.2.2 Scanning Vibrating Electrode Technology (SVET)

The scanning vibrating electrode technique (SVET) adopted the SVP100 test system produced by EG&G Company of the United States, and was used to measure the local current density in places

with artificial defects. The model of the platinum vibration probe was SOPC608, and the probe vibration amplitude was 30 μm . The scanning methods included the surface sweep and line sweep (equivalent to dividing the surface sweep area into several parts and testing one of the areas). The scanning speed was $800\mu\text{m}\cdot\text{s}^{-1}$, and the scanning area had a size of $8000\mu\text{m} \times 6000\mu\text{m}$. The sensitivity of probe SOPC608 was 1 mV and the step resolution was 0.5 micron. The output time constant of the phase-locked amplifier was 0.1s, and electrochemical sensitivity was less than $5\mu\text{A}\cdot\text{cm}^{-2}$. Before the measurements, artificial defect was formed on the coatings by using a circular drill with a bottom diameter of 6mm.

2.2.3 Scanning electron microscope (SEM)

The surface morphology of the coating was investigated using a XL30 scanning electron microscope (manufactured by Philips, Netherlands) with an accelerating voltage of 5 kV.

2.2.4 Atomic force microscope (AFM)

Atomic force microscopy (AFM) was conducted using an Asylum Research Cypher ES Atomic Force Microscope, and measurements were taken for each sample to measure surface topography.

2.2.5 Differential scanning calorimetry (DSC)

Differential scanning calorimetry (DSC) (Q2000, TA Instruments, USA) was carried out under nitrogen. The heating rate is $10^{\circ}\text{C}/\text{min}$, and the temperature varies from 0 to 250°C .

3. RESULTS AND DISCUSSION

3.1 Research on the curing technology of a composite coating

The key technology in the preparation of the coating is how to obtain the ideal self-stratifying effect. There are many factors that can affect the self-stratifying performance of the coating, including the composition ratio of the coating, the compatibility of the resin, the specific gravity of the coating particles, the modification effect of the additives on particle surface [21], the curing process of the coating and the preparation of the coating, etc [22,23].

In order to realise the best curing process of the coating, we first performed differential scanning calorimetry (DSC). Fig. 1 presents the DSC curve of the waterborne epoxy resin. The results show that the DSC curve from room temperature to 87.1°C was an endothermic curve, because the water molecules on the coatings evaporated after absorbing heat. Then, the curve flattened between 87.1°C and 106.1°C , during which water molecules evaporated completely, but the waterborne epoxy resin latex particles did not change. The coating started absorbing heat at 106.1°C and this peaked at 128.2°C . At this point, the water-based epoxy resin latex particles were heated into a molten state, making the resin to spread

horizontally in the space. As the temperature increased, some of the active groups in the polymer chain of the water-based epoxy resin started cross-linking and releasing heat, and this peaked at 185.0°C.

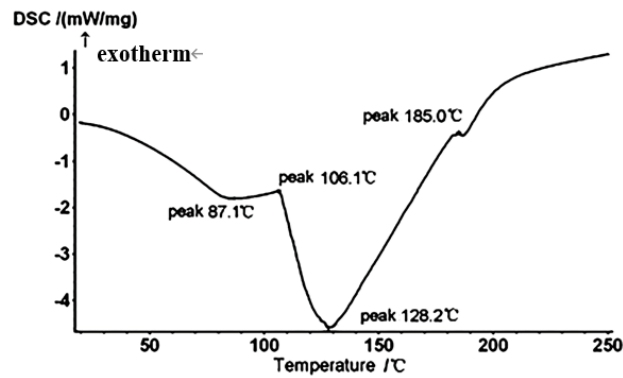


Figure 1. DSC curves of waterborne epoxy resin.

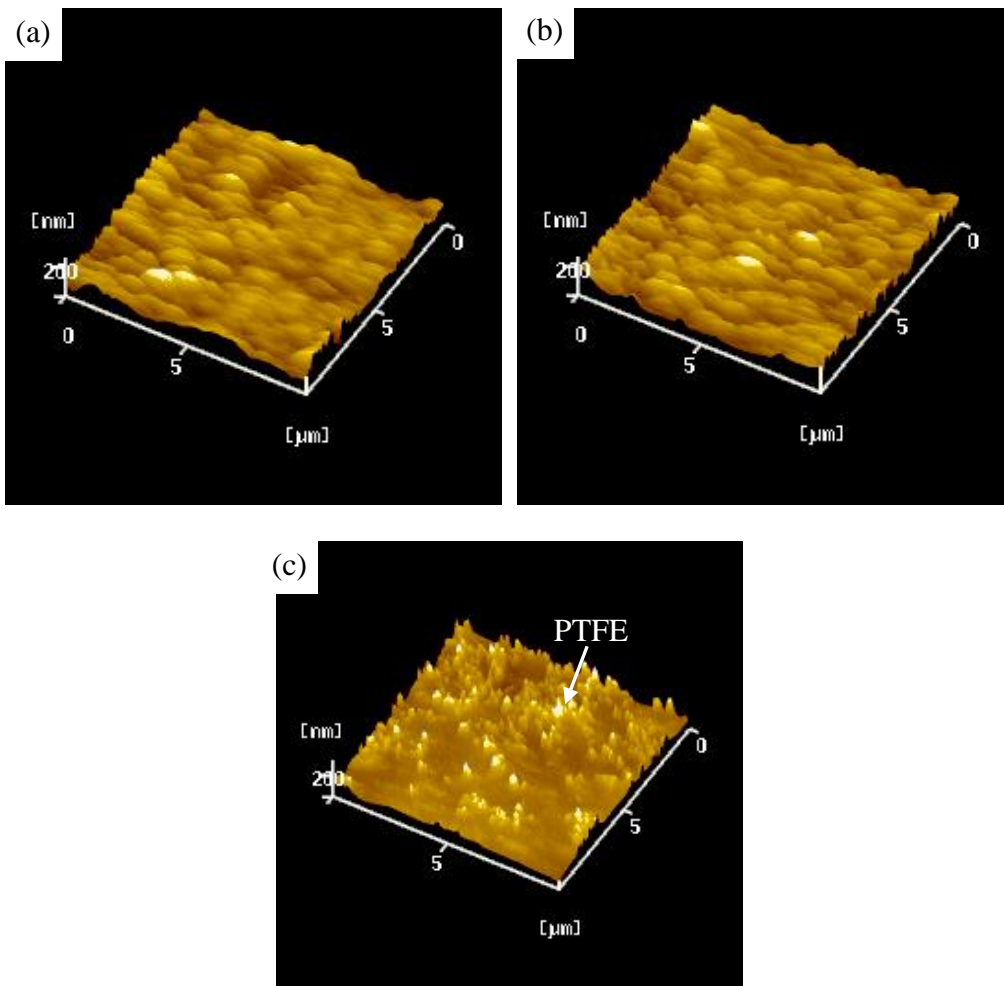


Figure 2. AFM surface topography images of the nano Al-PTFE modified coating with different curing processes: (a) directly drying at 200°C for 5 min, (b) firstly pre-drying at 50°C for 15 min and then drying at 200°C for 5 min, (c) firstly pre-drying at 110°C for 15 min and then drying at 200°C for 5 min.

Fig. 2 presents the AFM surface topography images of the nano Al-PTFE modified coating with different curing processes. Fig. 2(a) shows the image of the coating that was directly dried at 200°C for 5 minutes. The surface roughness of the coating can be attributed to the solvent evaporation during the curing period of the epoxy coating film, which led to the formation of some holes that reduced surface evenness. Since the epoxy resin cannot melt at 50°C, capillary pressure cannot be realised, and so the surface roughness of the coating in Fig. 2(b) is almost the same as that in Fig. 2(a).

However, the surface roughness of the coating in Fig. 2(c) is very high and appears to have a self-stratifying structure. The explanation for this phenomenon is that the epoxy resin latex particles in the coating melted at 110°C, which in turn generated capillary pressure causing the PTFE to protrude into the air and accumulate on the coating surface. Thus, PTFE can provide self-lubricating properties to the nano Al-PTFE modified coating, and so if it introduced on the coating surface, and it can help reduce the mechanical damage of the coating and also provide long-term corrosive protection [24]. Therefore, according to the results, the best curing process is pre-drying at 110°C and then drying at 200°C.

3.2 The electrochemical corrosion behaviour of the coating with artificial defects

3.2.1 EIS Study

Electrochemical Impedance Spectroscopy (EIS) was widely known as a test method to evaluate the corrosion resistance of coatings [25,26,27]. EIS was used to evaluate the corrosion resistance of pure waterborne epoxy coatings, nano Al modified coatings and nano Al-PTFE modified coatings, which immersed in 3.5% NaCl solution. Fig. 3 showed that compared to the other two coatings, the nano Al-PTFE modified coating had a lower capacitance and a higher resistance. For the other two coatings, the capacitive reactance arc radius gradually decreased, and the low-frequency impedance modulus continued to decrease, indicating that the corrosion resistance was not as good as the nano Al-PTFE modified coating.

Electrical Equivalent Circuit (EEC) analysis is generally used to interpret the impedance spectrum. To quantify the corrosion resistance of samples featuring a circular artificial defect with a diameter of 4 mm, immersed in 3.5wt. % NaCl solution, we built an EEC model to fit the EIS data, as shown in Fig. 4. The parameter values of double-layer capacitance C_{dl} and the charge transfer resistance R_{ct} obtained from the EEC model for the coatings immersed in 3.5 wt.% NaCl solution are shown in Table 1. At the initial immersion time, the nano Al-PTFE modified coating had a lower C_{dl} , but its R_{ct} was higher than that of the other two coatings, indicating that the corrosive electrochemical activity area of the Q235 steel was small. As the immersion time increased, R_{ct} firstly decreased and then formed a platform curve, and the value of the nano-Al PTFE modified coating was lower than that of the other two coatings. This indicates that the nano-Al PTFE modified coating had a lower rate of corrosion at the places with artificial defects.

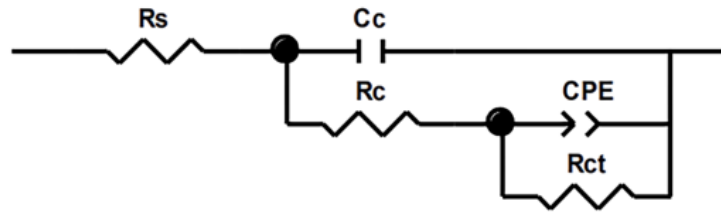


Figure 4. The EEC models for EIS analysis of the coatings.

3.2.2 SVET study

Fig 5. shows the SVET current intensity mapping of the three coatings. As Fig. 5(a) shows, for the waterborne epoxy coating, after 30 min of immersion in 3.5 % NaCl, the first scanning of the scratch was characterized by a high anodic current of $21.2 \mu\text{A}\cdot\text{cm}^{-2}$, which indicates the initialization of corrosion attack within the scratch. When immersed for up to 24 h, an obvious expansion of the electrochemical reactive zone and an increase of current density of $60.8\mu\text{A}\cdot\text{cm}^{-2}$ were observed. This indicates that the uniform corrosion of Q235 steel aggravated at the defective areas. However, for the nano Al modified coating and the nano Al-PTFE modified coating, much lower levels of anodic current density were observed at the initial immersion time, as shown in Fig. 5(b, c). The exposed artificial defect area became inactive and the corrosion was controlled by a cathodic process. This can be explained by the passivation of the nano Al to form $\text{Al}(\text{OH})_3$ to provide temporary protection [28].

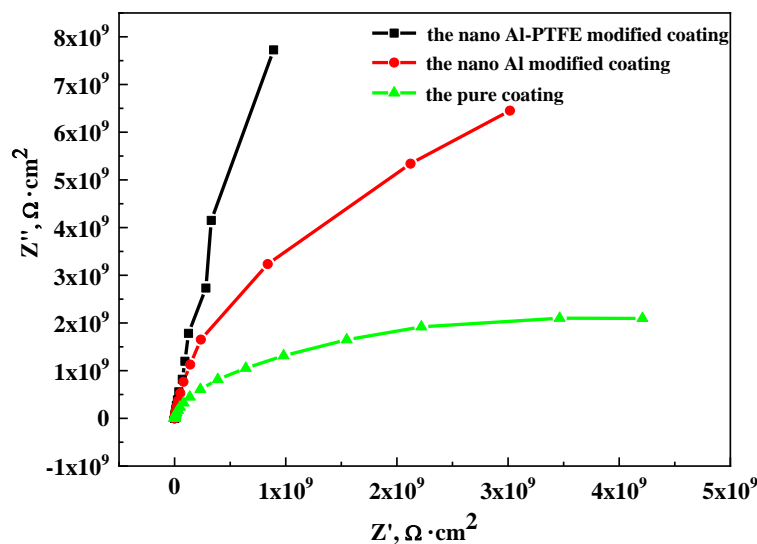


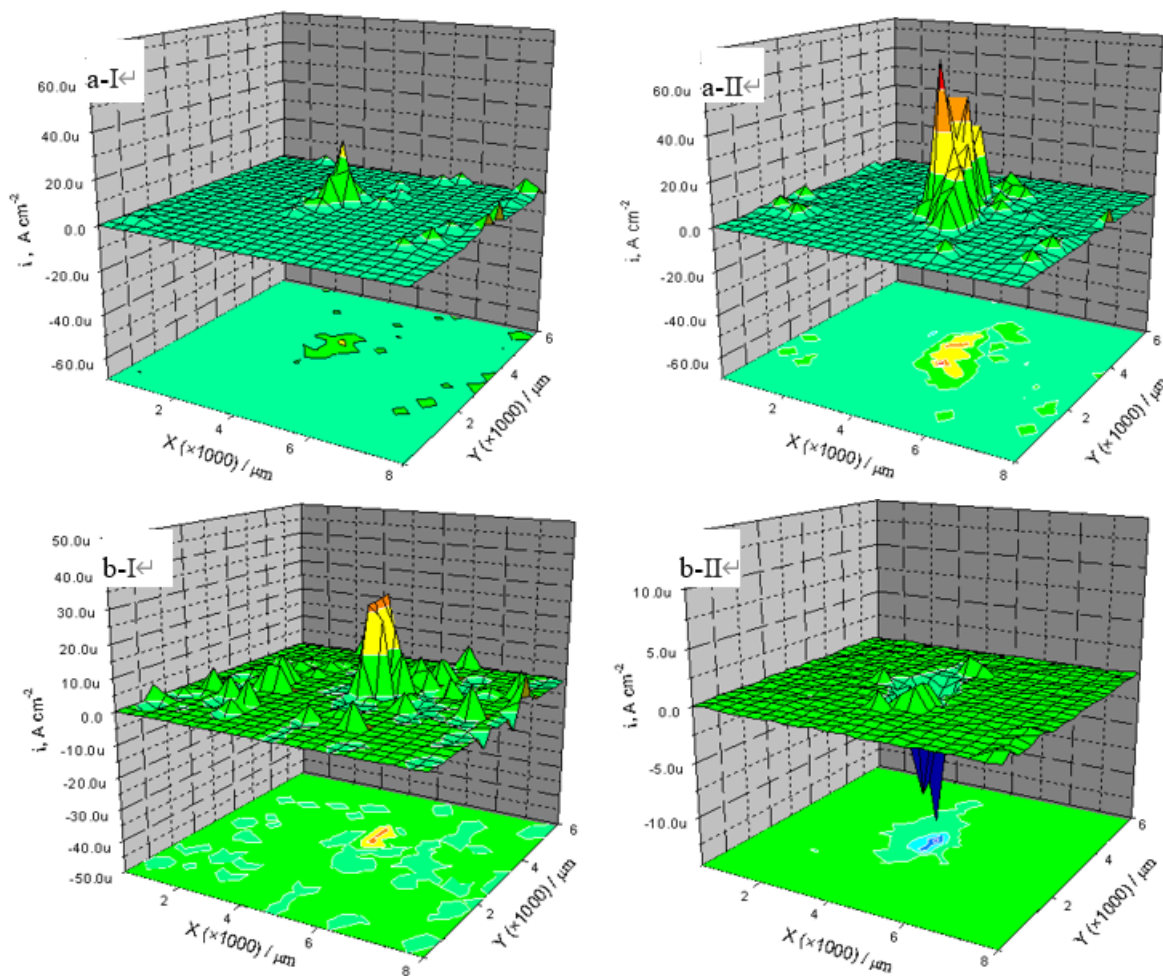
Figure 3. Nyquist plots of the pure waterborne epoxy coating, the nano Al modified coating and the nano Al- PTFE modified coating after 60 hours of immersion in 3.5% NaCl solution.

Fig. 6 shows the relationship between the coating current intensity and the distance from the defect edge profile for the three coatings. In Fig. 6(a), a significant expansion of electrochemical reactive region at the defective area can be observed, which indicates that the corrosion site reached the interface between the pure water-borne epoxy paint and steel after 48 h of immersion from the edge of the pure

artificial defect. Fig. 6(b) shows that the corrosion rate of the nano-Al modified coating had slowed down considerably, but corrosion was still far from the edge of the defect area after 48 h of immersion. However, Fig. 6(C) shows that there was little change in the distance of the nano Al-PTFE modified coating from the defect edge contour after 48 h of immersion. The results confirmed that nano-Al powder contributed to anti-corrosive performance by improving the wet adhesion of the coating and decreasing the expansion of corrosion under the coating.

Table 1. $\log C_{dl}$ and $\log R_{ct}$ value obtained from the EEC for the coatings immersed in 3.5wt. % NaCl solution.

| sample | $\log C_{dl} (F/cm^2)$ | | | | $\log R_{ct} (\Omega \cdot cm^2)$ | | | |
|---------------|------------------------|-------|-------|-------|-----------------------------------|------|------|------|
| | 0.5 h | 16 h | 32 h | 48h | 0.5 h | 16 h | 32 h | 48h |
| pure | -3.79 | -3.71 | -3.68 | -3.66 | 4.54 | 4.22 | 4.11 | 4.03 |
| nano Al | -4.13 | -4.18 | -4.07 | -4.04 | 5.08 | 3.69 | 3.80 | 3.79 |
| nano Al- PTFE | -4.99 | -4.31 | -4.10 | -3.94 | 5.38 | 4.49 | 3.33 | 3.39 |



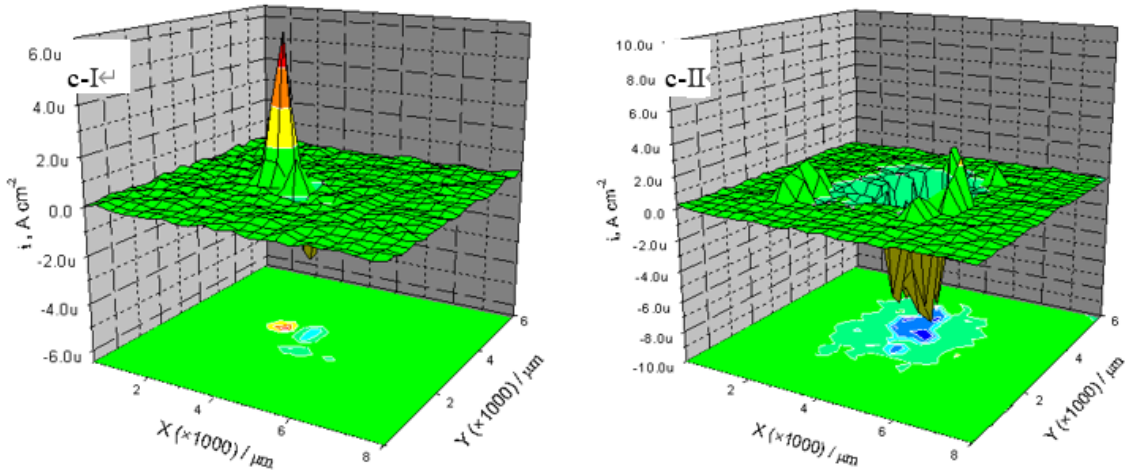
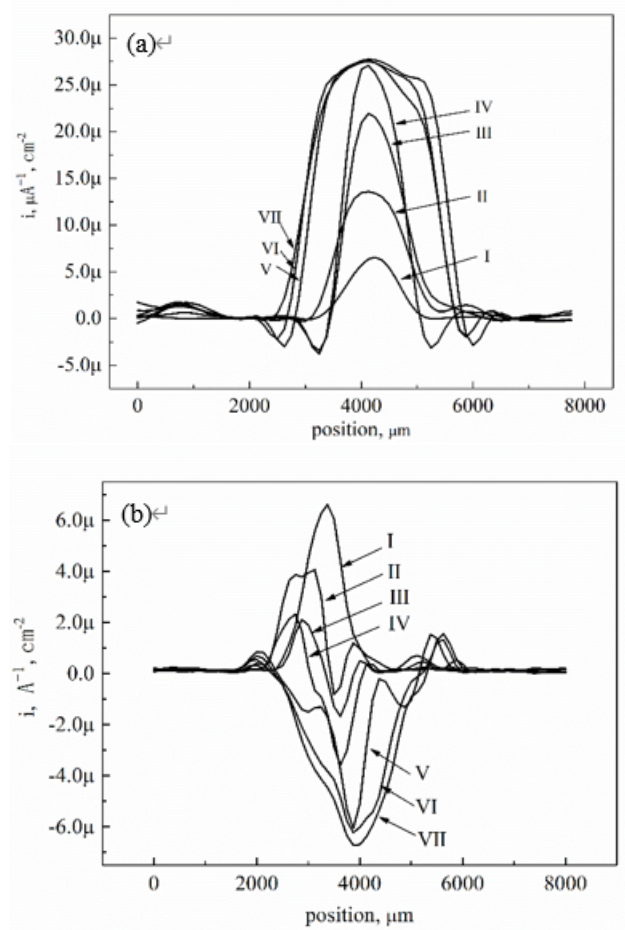


Figure 5. SVET current intensity mapping of the coatings: (a) the pure waterborne epoxy coating, (b) the nano Al modified coating and (c) the nano Al-PTFE modified coating at the artificial defect, immersed in 3.5wt.% NaCl solution for (I) 30 min and (II) 24 h.



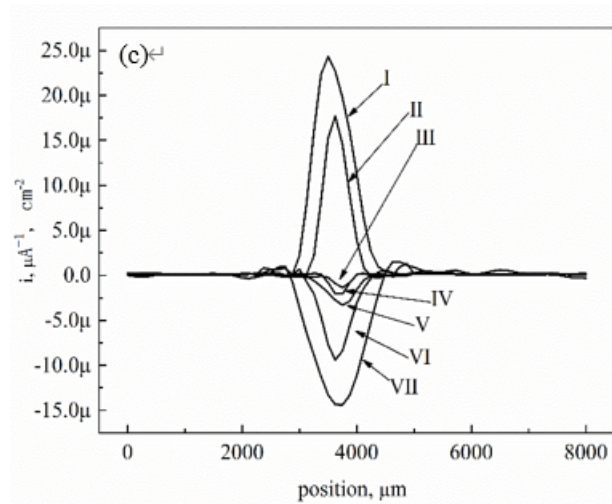


Figure 6. The relationship between the coating current intensity and the distance from the defect edge profile: (a) the pure waterborne epoxy coating, (b) the nano Al modified coating, (c) the nano Al-PTFE modified coating, immersed in 3.5wt.% NaCl solution for: (I)30 min, (II)8 h, (III)16 h, (IV)24 h, (V)32 h, (VI)40 h and (VII)48 h.

3.3 Evolution of coating capacitance C_c with immersion time

According to the equivalent circuit, the total impedance of the coating at this time can be obtained:

$$Z = R_s + \frac{R_s}{1+j\omega C_c R_c} = R_s + \frac{R_c}{1+\omega^2 C_c^2 R_c^2} - \frac{j\omega C_c R_c^2}{1+\omega^2 C_c^2 R_c^2} \quad (1)$$

Where ω represents angular frequency ($\omega = 2\pi f$, f is the frequency), and $j = \sqrt{-1}$. From Eq. (1), the imaginary part of the impedance is derived:

$$Z'' = -\frac{\omega R_c^2 C_c}{1+(\omega R_c C_c)^2} \quad (2)$$

At the high frequency, since $R_c \gg 1$, C_c can be calculated from the follow equation:

$$C_c = \frac{1}{2\pi f Z''} \quad (3)$$

When the coating was first immersed in 3.5% NaCl solution, the coating had strong anti-corrosion performance, so the impedance of the coating was very high. The samples tested at low frequencies were quite different from the actual results. But the imaginary part of the impedance at frequency was closer to reality [29]. In this study the capacitance is determined by the impedance value at about 10 kHz.

Fig. 7 shows the $\text{Log}C_c \cdot t^{1/2}$ curves of three different coatings immersed in 3.5% NaCl solution, where the coating capacitance (C_c) represents the water permeability of the coating. During the initial stage of immersion, the C_c value of the nano Al-PTFE modified waterborne epoxy coating was significantly higher than that of the other two coatings. However, after immersion for 100 h, the C_c of the nano Al-PTFE modified waterborne epoxy coating increased slower than that of the other two coatings. The results demonstrate that the nano-aluminum powder and the PTFE particles played a synergistic effect, effectively blocking the penetration of the electrolyte solution.

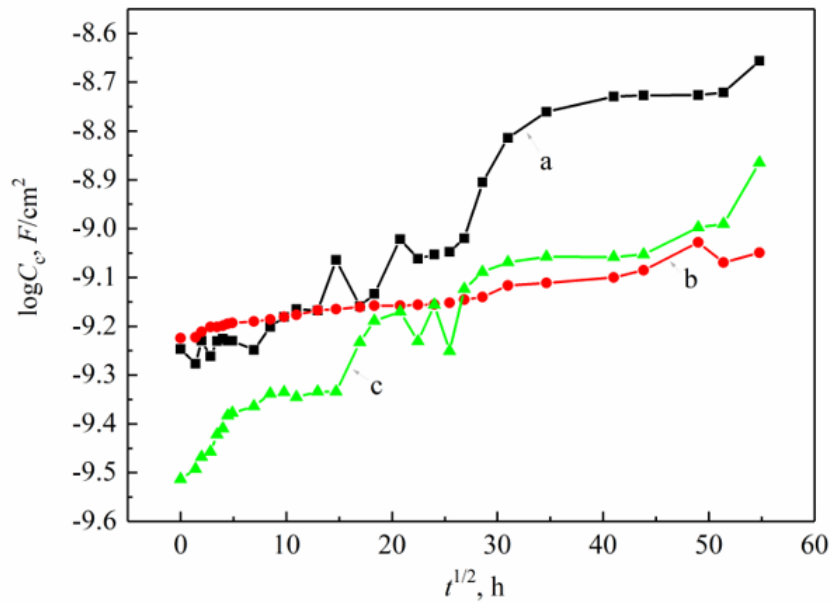


Figure 7. $\log C_c-t^{1/2}$ curves for three different coatings immersed in 3.5% NaCl solution: (a) the pure waterborne epoxy coating, (b) the nano Al modified coating and (c) the nano Al- PTFE modified coating.

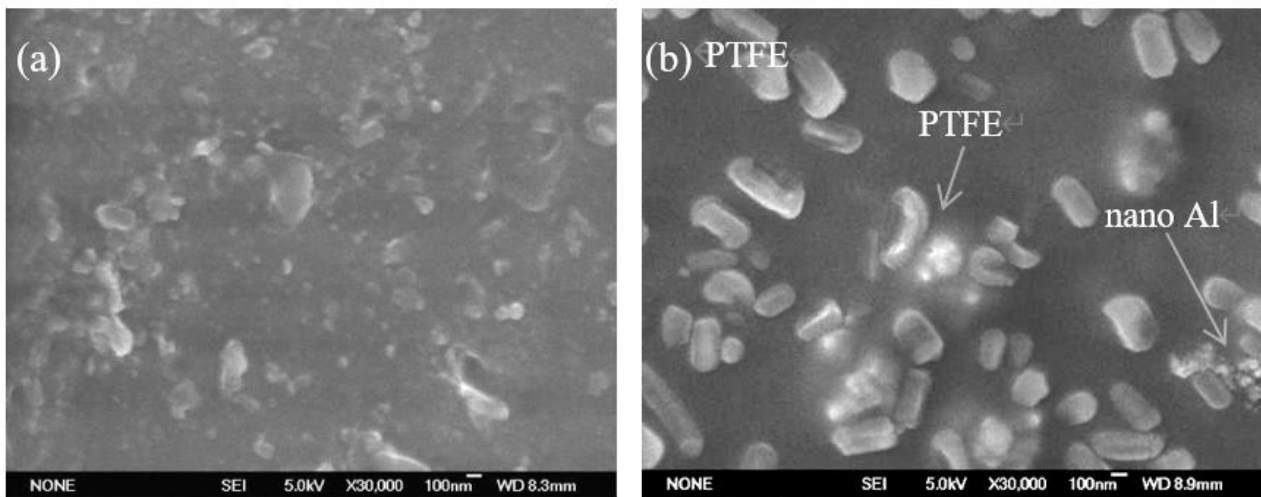


Figure 8. Surface morphology SEM images of the coatings: (a) the nano Al modified coating and (b) the nano Al- PTFE modified coating.

Fig. 8 shows the surface morphology of the nano Al modified coating and the nano Al-PTFE modified coating. The contents of the nano Al powder in the two coatings were same; however, more PTFE particles were deposited on the surface of the nano Al-PTFE modified coating. The results indicate that the PTFE particles deposited on the surface as well as the nano Al particles introduced in the substrate facilitated the formation of a self-stratifying structure of the coating during the curing process.

3.4 The analysis of the characteristic frequency (f_b)

The microscopic defects of the coating film accelerated the corrosion process of the substrate metals, and so the degree of deterioration of the protective coating can be known based on the size of the microscopic defect area. It has been proposed that the characteristic spectrum method can be used to analyse the defect area of the coating to determine the corrosion resistance of the coating [30]. The characteristic frequency f_b is the frequency point when impedance changes from capacitive to resistive behaviour.

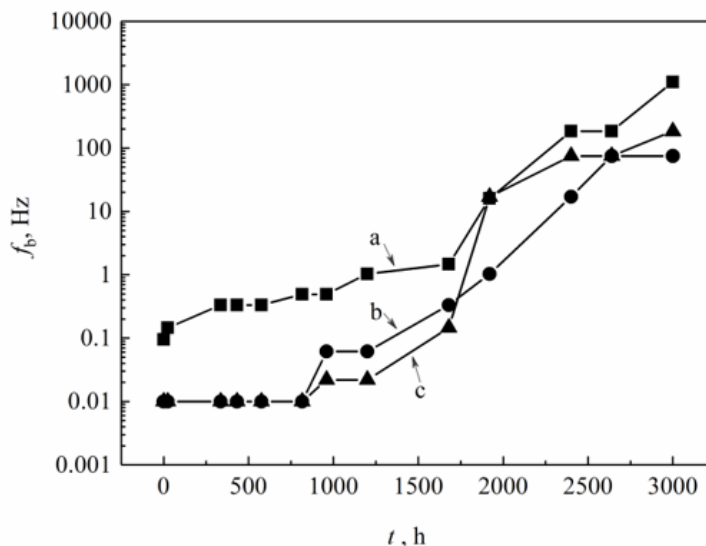


Figure 9. The characteristic frequency curves of three different coatings immersed in 3.5% NaCl solution: (a) the pure waterborne epoxy coating, (b) the nano Al modified coating, (c) the nano Al-PTFE modified coating.

The frequency corresponding to an inflection point on the $\log|Z|$ in the Bode plot and the inflection point on the $\log f$ curve is the characteristic frequency f_b and the corresponding phase angle is 45° . When the defect area is small at the initial stage of immersion, the main responses are the coating capacitance and the coating defect resistance. Additionally, the frequency when the coating capacitance is equal to the defect resistance R_c (ignoring the solution resistance R_s) is f_b , and is a direct function of the defect area (A_d). The relevant formulas are as follows:

$$R_c = \frac{1}{2\pi f_b C_c} \tag{4}$$

$$R_c = \frac{\rho d}{A_d} = \frac{\rho d}{PA} \tag{5}$$

$$C_c = \frac{\varepsilon \varepsilon_0 (A - A_d)}{d} \tag{6}$$

Where ρ is the defective coating, d is the coating thickness, ε is the dielectric constant of the aqueous coating, ε_0 is the dielectric constant of the dry film, A is the apparent measurement area, and P is the percentage of the area of failure.

When $A_d < 1\%$, $A - A_d \approx A$, then

$$f_b = \frac{A_d}{2\pi \varepsilon \varepsilon_0 \rho} = \frac{KA_d}{A} = KP \tag{7}$$

$$K = \frac{1}{2\pi\epsilon\epsilon_0\rho} \quad (8)$$

In general, as the coatings decay, the changes of ϵ and ρ are much smaller than the changes of f_b . When growth and loss cancel each other out, then K is a constant. Therefore, the changing rate of f_b can be used to determine the degree of coating failure.

Fig. 9 shows the characteristic frequency curves of the pure waterborne epoxy coating, the nano Al modified coating and the nano Al-PTFE modified coating. It can be seen that in the period before 1700 hours, the f_b of the nano Al-PTFE modified coating is lower than that of the other two coatings. After 1700 hours, the value of f_b rises rapidly, indicating that the defect area of the nano Al-PTFE modified coating is increasing. Looking at the whole immersion process, the f_b of the nano Al-PTFE modified coating was markedly lower than that of the nano Al modified coating. The results indicate that the pigments in the nano Al-PTFE modified coating and the nano Al modified coating effectively reduced microscopic defects, making it more difficult for the electrolyte to penetrate into the coating.

4. CONCLUSION

In this work, the nano Al and PTFE pigments were introduced into the waterborne epoxy resin to provide protection to the Q235 steel. Compared with the pure waterborne epoxy coating and the nano Al modified coating, the nano Al-PTFE modified coating provided not only anti-corrosion protection but also lubrication function due to its self-stratifying structure, which was formed by the introduction of nano Al particles in the substrate and the deposition of PTFE particles on the surface of the coating. The EIS and SVET results show that nano Al particles improve anti-corrosive performance by effectively blocking the penetration of the electrolyte solution into the coating, and by improving the wet adhesion to decrease the expansion of corrosion under the coating. In summary, the corrosion resistance of the nano Al-PTFE modified coating was significantly enhanced.

ACKNOWLEDGEMENTS

The authors acknowledge the financial support from the National Natural Science Foundation of China (No. 51401063), the Fundamental Research Funds for the Central Universities, China (3072020CF1003) and the Fundamental Research Funds for the Central Universities, China (3072020CF1003).

CONFLICTS OF INTEREST

No conflict of interest exists in the submission of this manuscript, and it is approved by all authors for publication.

References

1. J. A. Nardi, J. A. Strauss, F. M. Fardo, L. C. Ferreira, E. M. A. Martini, F. Horowitz, *Prog. Org. Coat.*, 148 (2020) 105823.
2. M. Kraljić, Z. Mandić, L. Duić, *Corros. Sci.*, 45 (2003) 181.
3. M. A. Hernandez, F. Galliano, D. Landolt, *Corros. Sci.*, 46 (2004) 2281.
4. N. S. Sangaj, V. C. Malshe, *Prog. Org. Coat.*, 50 (2004) 28.
5. Z. Ranjbar, S. Moradian, M. R. M. Z. Attar, *Prog. Org. Coat.*, 51 (2004) 87.
6. C. Le Pen, C. Lacabanne, N. Pébère, *Prog. Org. Coat.*, 39 (2000) 167.

7. A. P. Ordine, S. L. Díaz, I. C. P. Margarit, O. R. Mattos, *Electrochim. Acta*, 49 (2004) 2815.
8. M. A. Hernandez, F. Galliano, D. Landolt, *Corros. Sci.*, 46 (2004) 2281.
9. 9.G. Ji, L. F. Macía, B. Allaert, A. Hubin, H. Terryn, *J. Electrochem. Soc.*, 165 (2018) C246.
10. J. T. Zhang, J. M. Hu, J. Q. Zhang, C. N. Cao, *Prog. Org. Coat.*, 51 (2004) 145.
11. E. K. Melara, A. Z. Mendes, N. C. Andreczevecz, M. O.G.P. Bragança, G. T. Carrera, R. A. Medeiros-Junior, *Constr. Build. Mater.*, 242 (2020) 118001.
12. J. Hu, X. Li, J. Gao, Q. Zhao, *Mater. Design*, 30 (2009) 1542.
13. Sh. Montazeri, Z. Ranjbar, S. Rastegar, *Prog. Org. Coat.*, 111 (2017) 401.
14. S. Chen, B. Zhu, X. Liang, *Int. J. Electrochem. Sci*, 15 (2020) 1.
15. C. Wan, L. Zhang, X. Liu, *Int. J. Electrochem. Sci*, 15 (2020) 26.
16. S. Zhang, D. Cao, L. Xu, Z. Lin, R. Meng, *Int. J. Electrochem. Sci*, 15 (2020) 177.
17. T. Liu, J. Li, X. Li, S. Qiu, Y. Ye, F. Yang, H. Zhao, *Prog. Org. Coat.*, 128 (2019) 137.
18. J. H. Park, T. H. Yun, K. Y. Kim, Y. K. Song, J. M. Park, *Prog. Org. Coat.*, 74 (2012) 25.
19. L. L. Xue, L. K. Xu, Q. F. Li, *Mater. Sci. Forum*, 561 (2007) 2411.
20. A. Beaugendre, S. Degoutin, S. Bellayer, C. Pierlot, S. Duquesne, M. Casetta, M. Jimenez, *Prog. Org. Coat.*, 103 (2017) 101.
21. V. Verkholtantsev, M. Flaavian, *Prog. Org. Coat.*, 29 (1996) 239.
22. R. Hardis, J. L.P.Jessop, *Compos. Part A-Appl. S.*, 49 (2003) 100.
23. S.A. Haddadi, A. Ramazani, *Compos. Part B-Eng. J.*, 175 (2019) 107087.
24. Y. Chen, X. Lu, *Surf. Coat. Tech.*, 337 (2018) 379.
25. S.B. Lyon, R.Bingham, *Prog. Org. Coat.*, 102 (2017) 2.
26. M. Azadi, M.E. Bahrololoom, *Prog. Color Colorants Coat.*, 9 (2016) 53.
27. Z. Ranjbar, S. Montazeri, *Color Colorants Coat.*, 2 (2009) 23.
28. O. Ø. Knudsen, J. V. Bokhorst, *Corrosion*, 72 (2016) 560.
29. G.W.Walter, *Corros. Sci.*, 26 (1986) 681.
30. R. Hirayama, S. Haruyama, *Corros. Sci.*, 47 (1991) 952.